

Decoherence induced by a chaotic environment: A quantum walker with a complex coin.

Leonardo Ermann,^{1,2} Juan Pablo Paz,^{2,3} and Marcos Saraceno^{1,4}

¹*Departamento de Física, Comisión Nacional de Energía Atómica. Avenida del Libertador 8250 (C1429BNP), Buenos Aires, Argentina.*

²*Departamento de Física, FCEyN, UBA, Pabellón 1 Ciudad Universitaria, 1428 Buenos Aires, Argentina.*

³*Theoretical Division, LANL, MSB213, Los Alamos, NM 87545, USA*

⁴*Escuela de Ciencia y Tecnología, Universidad Nacional de San Martín. Alem 3901 (B1653HIM), Villa Ballester, Argentina.*

(Dated: 16th October 2018)

We study the differences between the process of decoherence induced by chaotic and regular environments. For this we analyze a family of simple models which contain both regular and chaotic environments. In all cases the system of interest is a “quantum walker”, i.e. a quantum particle that can move on a lattice with a finite number of sites. The walker interacts with an environment which has a D dimensional Hilbert space. The results we obtain suggest that regular and chaotic environments are not distinguishable from each other in a (short) timescale t^* , which scales with the dimensionality of the environment as $t^* \propto \log(D)$. However, chaotic environments continue to be effective over exponentially longer timescales while regular environments tend to reach saturation much sooner. We present both numerical and analytical results supporting this conclusion. The family of chaotic evolutions we consider includes the so-called quantum multi-baker-map is a particular case.

PACS numbers:

I. INTRODUCTION

The study of the transition from quantum to classical physics began with the rise of quantum mechanics itself [1]. In recent years it became clear that the process of decoherence plays an essential role in understanding this transition [2]. According to this modern view, classicality is an emergent property that is induced on sub-systems due to the interaction with their environment. Decoherence is not only important from a fundamental point of view but also its understanding seems to be crucial to develop new quantum technologies such as quantum computation [3]. The role of the environment is essential in the process of decoherence. In fact, this process can be understood as the consequence of the dynamical creation of quantum correlations (entanglement) between the system and its environment. Due to this process, all quantum information initially present in the state of the system is lost in the correlations with the environment, which effectively measures the state of the system. Due to this process, the vast majority of the quantum states in the Hilbert space of the system become highly unstable. Only the small subset of states that are relatively immune to the interaction with the environment (the so-called pointer states) remain relatively stable.

In studies of decoherence the environment is usually modelled in a simple way using a phenomenological approach. In fact, the best known such model is the bosonic bath, where the environment consists of an infinite number of harmonic oscillators [4, 5, 6]. Although it is well known that this model is not universally applicable [7] it captures many of the essential ingredients of the decoherence process and it is quite adequate to describe the interaction between quantum systems and large reservoirs which are near some equilibrium state. Spin baths have been also studied and display some distinctive features [8, 9, 10].

Recently, interest in the study of the effect of the intrinsic complexity of the environment on decoherence arose. In fact, there is some evidence that chaotic environments may induce decoherence more effectively than regular ones [11].

A particular manifestation of this higher effectiveness may be the dependence of the decoherence timescale on the system-environment coupling strength λ : regular environments induce a decoherence rate which is roughly proportional to λ^2 while unstable [11] or chaotic [9] environment may display a much weaker dependence with λ . On the other hand, issues such as the heat capacity of a chaotic system as a reservoir have been addressed [12] and also point at a significant difference between the way in which chaotic and regular systems can act as effective reservoirs.

In this paper we will present a study of the evolution of a quantum system coupled to an environment which will be chosen from a family containing both chaotic and regular representatives. The model we will analyze has recently attracted some attention in the context of studies of quantum information processing. Thus, we will consider the evolution of a quantum walker (a quantum particle moving on a finite lattice). The quantum walker carries a quantum coin which usually consists of a spin 1/2 particle. The direction of the motion of the walker is conditioned on the state of the quantum spin. Here, we will consider that the quantum coin is part of a larger quantum system with which it interacts by means of a unitary operator with either chaotic or regular properties (see below). The usual quantum walk has been studied recently as a potentially useful quantum sub-routine [13] and the impact of the process of decoherence has also been discussed using a variety of tools [14, 15].

We will use a family of unitary operators to define the evolution of the environment. This family was introduced some time ago for a system of qubits [16] and contains a fully integrable member (in such case each qubit evolves independently of the others, each of them acting as independent coins [17]) and other unitary operators which can be seen as the quantization of chaotic systems. The family includes the conventional “quantum baker’s map” which is perhaps the simplest and most studied chaotic unitary map [18, 19]. In such case, the complete system we analyze is a variant of the so-called quantum multibaker chain, which was analyzed before in a

different context [20].

In our paper we will analyze the behavior of the system (the walker) and show how the interaction with the environment induces classical behavior on it. We will point out some differences between the effects induced by the environment when its dynamics is chaotic and regular. Our model has a drawback: It does not contain a parameter controlling the strength of the interaction between the system and the environment. Thus, we cannot detect effects such as the ones analyzed in [11]. However, our model will certainly help us to display striking differences between regular and chaotic regimes as a function of the dimensionality (D) of the Hilbert space of the environment. As we will see, regular and chaotic environments show some clear differences in their behavior after relatively short times.

The paper is organized as follows: In Sec. II we introduce the essential ingredients of the model we study. We describe the simplest quantum walk on the line and we discuss how it can be coupled to a variety of environments whose evolution belongs to the family of the quantum baker maps. In Sec. III we show numerical results for the evolution of the system. We analyze first the entropy induced by the interaction with the environment, which is the magnitude that displays more clearly the difference between the chaotic and regular maps. We also analyze the variance of the quantum walker and the distance between the phase space representation of the quantum walker and their classical counterparts. We present our conclusions in Sec. IV.

II. THE SYSTEM AND THE ENVIRONMENT

A. The system: a quantum walker on a ring.

We will consider a quantum walker that moves on a ring. The evolution will be defined by means of a sequence of unitary operations (discrete time). Let \mathcal{H}_P be the Hilbert space of the walker, which has a finite number of localized states $|j\rangle$ forming a basis that can be denoted as $\{|j\rangle; j = 0, \dots, M-1\}$. The case of an infinite line (i.e. $M \rightarrow \infty$) is interesting and, for initially localized states of the walker, can be obtained from our results for times that do not exceed $M/2$. If the walker carries a quantum coin consisting of a spin $1/2$ particle, the total Hilbert space is $\mathcal{H} = \mathcal{H}_P \otimes \mathcal{H}_C$ where \mathcal{H}_C is the space of states of the spin which is spanned by the two states $\{|0\rangle, |1\rangle\}$.

The evolution of the quantum walker is defined as the successive application of a unitary transformation which is itself built in two steps: First, we apply a unitary operator $(\hat{I}_P \otimes \hat{C}_C)$, which acts non-trivially on the coin-space (being the analogue of the classical ‘coin-flip’). Then, we apply an operator that translates the state of the walker to the left or to the right depending on the state of the quantum coin. So, the total evolution in one time-step is defined as

$$|\Psi(t+1)\rangle = \hat{U}^{\sigma_z} (\hat{I}_P \otimes \hat{C}_C) |\Psi(t)\rangle \quad (1)$$

where the translation operator \hat{U} acts on the space of the

walker (as $\hat{U}|j\rangle = |j+1\rangle$) and σ_z is the usual Pauli matrix acting in coin space. For the circle \hat{U} is diagonal in a basis which is obtained from the position states $|j\rangle$ by means of the usual discrete Fourier transform. This is the momentum basis defined as $|k\rangle = \frac{1}{\sqrt{M}} \sum_{j=0}^{M-1} \exp(-i\frac{2\pi jk}{M}) |j\rangle$. It can be easily shown that $\hat{U}|k\rangle = e^{-i\frac{2\pi k}{M}} |k\rangle$. The usual choice for the operator C_C , that defines the coin flip, is the so-called Hadamard transformation H , whose matrix in the $\{|0\rangle, |1\rangle\}$ bases is

$$H = \frac{1}{\sqrt{2}} \begin{pmatrix} 1 & 1 \\ 1 & -1 \end{pmatrix} \quad (2)$$

In this work we will enlarge the ‘coin’-space which will consists of N qubits instead of a single one. In this case the $D = 2^N$ -dimensional Hilbert space of the bigger coin will be denoted as \mathcal{H}_B and the total Hilbert space of the combined walker-coin system is $\mathcal{H} = \mathcal{H}_P \otimes \mathcal{H}_B$. At any single instant one qubit (which we denote as the ‘most significant qubit’ or MSQ) will determine the direction of the motion of the walker in the same way as in the ordinary quantum walk. However, we will consider the possibility that the evolution of the complex D -dimensional coin contains interactions between the different qubits. Thus, we can think this model as consisting of an ordinary quantum walk with a spin $1/2$ coin which interacts with extra degrees of freedom (in a way that will be specified below). A simple quantum circuit describing the evolution is shown in Figure 1. The operator $B_{N,n}$ defines the evolution of the complex coin and will be described in the next sub-section.

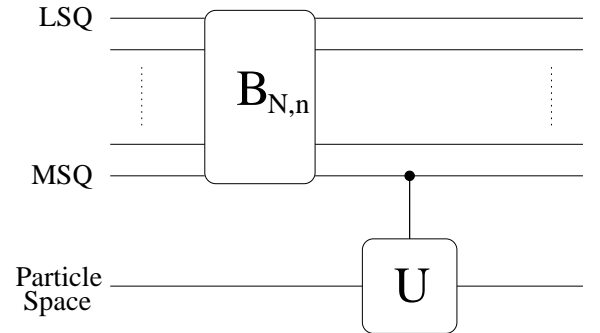


Figure 1: Circuit representation of the Quantum Walk interacting with families of Quantum Baker Maps

More formally, the evolution of the complete system is

$$\rho(t) = \hat{M}^t \rho(0) \hat{M}^{\dagger t} \quad (3)$$

where $\hat{M} = (\hat{U} \otimes \hat{P}_{0\ MSQ} + \hat{U}^\dagger \otimes \hat{P}_{1\ MSQ}) (\hat{I} \otimes \hat{B}_{N,n})$. The operators $P_{0\ MSQ}$ and $P_{1\ MSQ}$ are respectively the projectors onto the states $|0\rangle$ and $|1\rangle$ of the space of the most significant qubit. As mentioned above, the operator defining the evolution on the internal space of the complex (multi-qubit) coin is given by $\hat{B}_{N,n}$ which is described below.

To study the temporal evolution generated by the operator \hat{M} it is convenient to use the momentum basis for the quantum walker. Thus, as the translation operator \hat{U} is diagonal in such basis we only need to analyze the effect of the operator M_k , which being defined as $\langle k|M|k' \rangle = \delta_{k,k'} M_k$, acts in the Hilbert space of the complex coin and has the following matrix form:

$$\hat{M}_k = \begin{pmatrix} e^{-i\varphi_k} & 0 \\ 0 & e^{i\varphi_k} \end{pmatrix} \hat{B}_{N,n} \quad (4)$$

where the first term of the right side is a block-diagonal $D \times D$ matrix and $\varphi_k = \frac{2\pi k}{M}$.

B. The environment: a family of quantum baker's maps.

As we mentioned above, our complex coin consists of a set of N qubits. In the D -dimensional Hilbert space we will consider the temporal evolution induced by a family of evolution operators which were introduced and studied before [16, 21]. To define these operators it is convenient first to introduce the partial Fourier transform \hat{G}_n as the operator

$$\hat{G}_n \equiv \hat{I}_{2^n} \otimes \hat{F}_{2^{N-n}}^{\eta,\kappa}, \quad n = 0, \dots, N \quad (5)$$

where \hat{I}_{2^n} is the identity operator on the first n qubits, and $\hat{F}_{2^{N-n}}^{\eta,\kappa}$ is the Fourier transform on the remaining qubits. Matrix elements of this operator are defined (in terms of the so-called Floquet angles η and κ) as

$$\langle k|\hat{F}_D^{\eta,\kappa}|j \rangle = \frac{1}{\sqrt{D}} \exp(-i\frac{2\pi}{D}(j+\eta)(k+\kappa)). \quad (6)$$

We define a family of evolution operators which are parametrized by n (the number of qubits which are not affected by the partial Fourier transform) and also by the Floquet angles η and κ . To simplify the notation the dependence on these two parameters will be implicit from here on. The family consists of the operators $\hat{B}_{N,n}$ defined as (see [16]):

$$\hat{B}_{N,n} \equiv \hat{G}_{n-1}^{-1} \hat{S}_n \hat{G}_n \quad (7)$$

where the Shift operator \hat{S}_n acts only on the first n qubits and is such that: $\hat{S}_n|x_1\rangle|x_2\rangle \dots |x_n\rangle|x_{n+1}\rangle \dots |x_N\rangle = |x_2\rangle \dots |x_n\rangle|x_1\rangle|x_{n+1}\rangle \dots |x_N\rangle$.

There is a simpler expression for these operators that can be obtained using the fact that the shift \hat{S} commutes with \hat{G}_n . Then, $\hat{B}_{N,n}$ can be written as

$$\hat{B}_{N,n} = (\hat{I}_{2^{n-1}} \otimes \hat{B}_{N-n+1,1}) \circ \hat{S}_n. \quad (8)$$

Thus, the action of $\hat{B}_{N,n}$ is equivalent to a shift of the n left-most qubits followed by application of the map $\hat{B}_{N-n+1,1}$, which acts only on the $N-n+1$ least significant qubits. The map $\hat{B}_{N-n+1,1}$ is well known in the context of the study of quantum chaos. In fact, as the shift \hat{S}_1 is the identity, we have

$\hat{B}_{N,1} = \hat{F}_D^{-1} \circ (\hat{I}_2 \otimes \hat{F}_{D/2})$. Indeed, this map was introduced some time ago by Balasz, Voros and Saraceno as a quantization of the classical baker's map [18, 19]. For this reason, it will be denoted as B_{BVS} . The above equivalence is shown in circuit representation in figure 2.

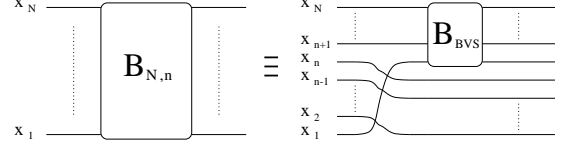


Figure 2: Circuit representation of the operator $\hat{B}_{N,n}$ in terms of the Balasz, Voros and Saraceno baker's map.

On the other hand, it is easy to show that $\hat{B}_{N,N}$, the extreme member of the family (obtained when $n = N$) is a map constructed only with swaps and single qubit Fourier transform. Some properties of this family of operators (such as their entangling power) were studied in [21]. It is interesting to point out that these maps can also be viewed as members of an even larger family where each member is a product of only two quantized iterations of the classical baker map [22]. The spectral properties of the maps are interesting. In fact, as will be discussed in detail elsewhere [22] all the members of the family have rather “chaotic” spectra while the only truly regular member is the extreme case $\hat{B}_{N,N}$ where every qubit evolves independently of the rest.

It is worth commenting on some aspects of the relation between the map $\hat{B}_{N,1}$ and the quantum version of the classically chaotic baker's map. In fact, the quantization of the baker's map can be done on an even-dimensional Hilbert space taking advantage of some very simple features of its classical counterpart. Thus, the classical baker's transformation acts on a phase space which is the unit square acting on position and momentum coordinates according to

$$q_{i+1} = 2q_i - [2q_i] \quad (9)$$

$$p_{i+1} = (p_i + [2q_i])/2 \quad (10)$$

where $[q]$ denotes the integer part of q . This map is an example of an intuitive geometrical transformation which stretches the square by a factor of two in the q direction, squeezes by a factor of a half in the p direction, and then stacks the right half onto the left. Another advantage of this map is that it has a simple symbolic dynamics using the binary *Bernoulli shift*. Writing both q and p in binary as $q = 0.\epsilon_0\epsilon_1\dots = \sum_{k=0}^{\infty} \epsilon_k 2^{-k-1}$ and $p = 0.\epsilon_{-1}\epsilon_{-2}\dots = \sum_{k=1}^{\infty} \epsilon_{-k} 2^{-k}$ ($\epsilon_i \in \{0,1\}$), every phase space point can be represented by a bi-infinite symbolic string as

$$(p, q) = \dots \epsilon_{-2}\epsilon_{-1}\epsilon_0 \bullet \epsilon_0\epsilon_1\epsilon_2\epsilon_3\dots \quad (11)$$

Then, the action of the baker's map upon symbols turns out to be

$$(p, q) \longrightarrow (p', q') = \dots \epsilon_{-2}\epsilon_{-1}\epsilon_0 \bullet \epsilon_1\epsilon_2\epsilon_3\dots \quad (12)$$

Thus, baker's map is a Bernoulli shift (notice that the most significant bit of the new momentum coordinate is inherited

from the most significant bit of position). Using this property, unitary operators that are quantizations of this classical map were defined [18, 19]. The basic idea is to use the unitary operator that maps position bases onto the momentum bases and let one qubit go through before applying the inverse transformation. Thus, the quantum version of baker's map is $\hat{B}_{BVS} = \hat{F}_D^{-1} \circ (\hat{I}_2 \otimes \hat{F}_{D/2})$.

It is clear that baker's map can be defined whenever the dimension of the Hilbert space is even. Moreover, it is well known that although the unitary operator has the spectral properties characterizing chaotic maps, the case of $D = 2^N$ has some peculiar features (where quasi-degeneracies occur?). In the coming section we will analyze the properties of an environment with a D dimensional Hilbert space in which one of the above operators generate the temporal evolution. In some cases we will also compare our results with an environment with an even dimensional Hilbert space (which is not a power of 2 but is close to one such power).

III. RESULTS: REGULAR AND CHAOTIC ENVIRONMENTS.

We will assume that the initial state of the combined “walker-coin” system is a tensor product of a localized state for the walker (which from now on will be denoted simply as “the particle”) and a pure state of the complex coin: $|\Psi_0\rangle = |0\rangle \otimes |\Phi_0\rangle = \sum_1^M \frac{1}{\sqrt{M}} |k\rangle \otimes |\Phi_0\rangle$. We study the reduced density matrix of the particle obtained by tracing out over the coin subspace. The evolution of the probability distribution of the particle is

$$p(x, t) = \frac{1}{M} \sum_{k, k'} \exp(-i \frac{2\pi}{M} x(k - k')) \langle \Phi_0 | \hat{M}_k^{\dagger} \hat{M}_{k'}^t | \Phi_0 \rangle \quad (13)$$

In the case of the classical random walk, $p(x, t)$ has the form of a binomial distribution with a width which spreads as \sqrt{t} .

A. Entropy production.

As the particle and its environment become entangled during the temporal evolution, the reduced density matrix of the particle loses its purity. A measure of the entanglement between the two subsystems (particle and coin) is the von Neumann entropy (S_V) computed from the reduced density operators. For simplicity, we will use instead the linear entropy defined as $S_L = -\log(\text{Tr}[\rho_P^2])$ which is easier to calculate and provides a lower bound to S_V . S_L varies between $S_L = 0$ for pure states and $S_L = \ln D$ for totally mixed states (where D is the dimension of the Hilbert space). It is worth mentioning that due to the fact that we choose the total state to be pure, the entropy of both subsystems is identical and is therefore limited by the minimum Hilbert space dimension (which we assume to be given by D as we are interested in considering the infinite line limit).

The entropy growth measures the transfer of quantum information from the initial state of the system onto the quantum

correlations with its environment. As mentioned above, at any given instant, the entropy measures the number of orthogonal states which are explored in the course of the evolution of both the system and the environment. For this reason, we expect to observe a difference on the entropy production power of chaotic and regular environments. The argument leading to this conclusion may be understood as follows: Two different localized states of the system can be viewed as generating two different effective evolutions for the environment. If the evolution is generated by a chaotic unitary map, it is known to exhibit extreme sensitivity to perturbations [23, 24]. Then, two different localized states of the particle will tend to correlate rapidly with approximately orthogonal states of the environment. Then, the entropy will grow until all available orthogonal directions in Hilbert space are explored. Therefore, for chaotic environments one expects the entropy to saturate at levels which are of the order of $\log(D)$. For regular environments one expects to be in the opposite regime: the evolution will tend to explore a number of dimensions which should be much smaller than in the chaotic case.

The time dependence of the linear entropy S_L is displayed in Figure 3 for some representative members of the family of environmental evolutions $B_{7,n}$ (we show the results corresponding to $\eta = \kappa = 0.5$, but the behavior is qualitatively similar for other Floquet angles).

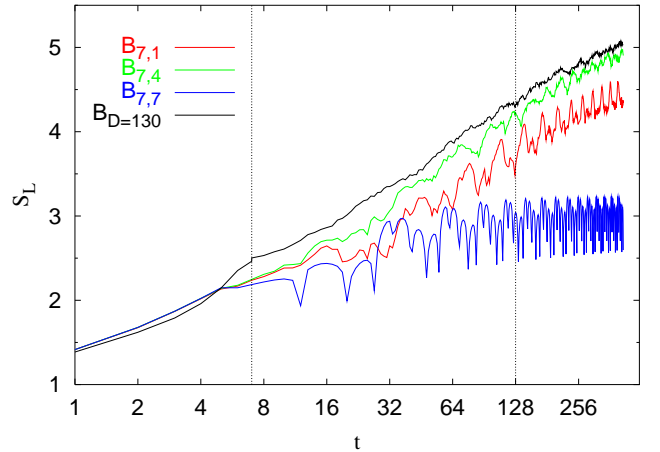


Figure 3: Linear entropy as a function of time for an environment of seven qubits evolving with some typical unitary operators of the family $B_{7,n}$. Floquet angles are fixed at $\eta = \kappa = 0.5$. The initial state of the particle is localized in position and the initial state of the environment was chosen as $\frac{1}{\sqrt{2}}(|0\rangle + i|1\rangle)$ for each qubit. Results are shown for a similar initial state for an environment with a $D = 130$ dimensional Hilbert space evolving with the baker's map (black line).

It is clear that a very different behavior is observed for the regular member of the family (the map $B_{N,N}$). In such case the entropy production saturates at a level which is of the order of $S_0 = \log(\log(D))$ (as $D = 128$ this value is close to $S_0 \approx 2.8$, see below). This behavior is also seen to be independent of the initial condition. As mentioned above, this can be understood as a consequence of the small generation of

entanglement between the qubits of the environment. On the other hand, all the other members of the baker's family $B_{N,n}$ for $n = 1, \dots, N-1$ have a similar behavior. The entropy continues growing approaching an asymptotic value which is of the order of a fraction of $\log(D)$. Entropy continues growing for times which scale proportionally to D , the Hilbert space dimensionality. It is worth mentioning that within the family of maps $B_{N,n}$ the ones that achieve maximal entropy growth correspond to intermediate values of n , in agreement with the results obtained in [21]. The fact that the maximal value of $\log(D)$ is not attained can be attributed to the quasi-degeneracies present in the spectrum of the baker's map for dimensions which are a power of two. In fact, in Figure 3 we also show the entropy production from a chaotic environment whose Hilbert space dimension is $D = 130$ (which is an even number close to a power of two). It is clear that the entropy for this map is larger than the rest. This supports the argument stating that an environment that is more chaotic is able to generate more entropy. It is also consistent with the claims of [21] concerning the fact that spatial symmetries in the quantum baker's map are responsible for deviations from the predictions of random matrix theory.

The behavior of the regular environment $\hat{B}_{N,N}$ can be examined using analytic tools. In fact, we can show that after the Ehrenfest time $\log(D)$ the linear entropy S_L oscillates around the saturation value S_0 with period which is identical to the number of qubits N . In fact, we can obtain a universal curve for the normalized linear entropy (S_L/S_0) as a function of the rescaled time t/N . This is shown in Figure 4.

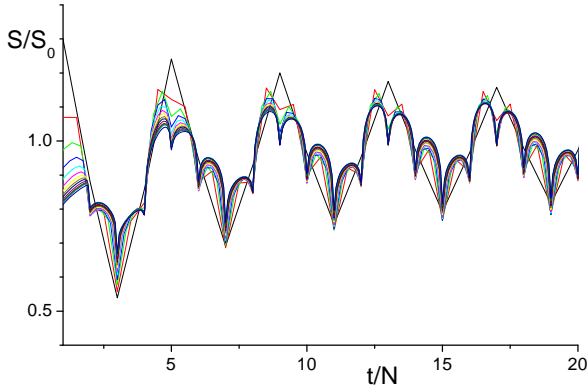


Figure 4: Linear entropy normalized vs t/N for many coins walk, $B_{N,N}$ and $\eta = \kappa = 0$, up to $N = 8$. The particle was localized in position and the initial state of the environment is $\frac{1}{\sqrt{2}}(|0\rangle + i|1\rangle)$ for each qubit

It is also possible to obtain a good estimate for the saturation value of the linear entropy. This is shown in Figure ?? where the behavior of S_0 (the saturation value of S_L) as a function of the number of qubits N is displayed. This saturation value is bounded by $\log(N)$ (which in turn implies that the linear entropy for regular environment is bounded by $\log(\log(D))$). In the above discussion we referred to the many-coin map as a regular system. The reason for our use of this terminology is the following: As the coins do not inter-

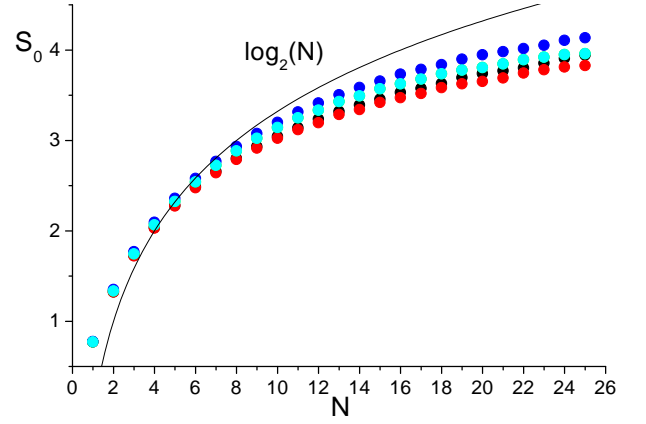


Figure 5: (Color on-line) Saturation value of linear entropy for many coins walk vs. number of coins. The initial state for each coin is $|\psi_0\rangle = |0\rangle$ (black), $|\psi_0\rangle = \frac{1}{\sqrt{2}}(|0\rangle + e^{i\frac{3\pi}{4}}|1\rangle)$ (red), $|\psi_0\rangle = \frac{1}{\sqrt{2}}(|0\rangle + i|1\rangle)$ (blue) with $\eta = \kappa = 0$. As argued in the text, the $\log(\log(D))$ curve establishes an upper bound for the saturation.

act the spectrum of the evolution operator is highly degenerate. It is worth mentioning that this is the only sense in which this can be viewed as an integrable system since it does not have a classical analogue.

B. Quantum and classical behavior of the spread of the wave-packet.

The study of the variance of the particle's position, that can be defined as $\sigma^2 = \langle x^2 \rangle - \langle x \rangle^2$ can be useful to signal the transition from a classical to a quantum regime. From the above study of the entropy we expect that both chaotic and regular systems should be quite efficient to enforce classical behavior for times which are of the order of $\log(D)$ (the Ehrenfest time). For larger times one expects regular environments to lose its ability to induce classicality. Thus, for larger times one expects the particle to spread according to the quantum predictions while for shorter times it should behave classically (although at first sight this may sound counter-intuitive, for this system one really expects to see a classical-to-quantum transition!). For the classical random walk, it is well known that the variance grows diffusively (i.e., linearly with time). In turn, for the ordinary quantum walk (with no decoherence mechanism) the variance grows quadratically with time. In figure 6 we show the standard deviation (σ) as a function of time for some representative members of the $B_{7,n}$ family (again, we display results for $\eta = \kappa = 0.5$ and for an initial state of the complex coin which is a tensor product of $\frac{1}{\sqrt{2}}(|0\rangle + i|1\rangle)$ for each qubit).

As expected, the standard deviation (SD) grows diffusively for short periods of time both for regular and chaotic environments. This is seen in the inset of Figure 6 where no noticeable difference between chaotic and regular environments arise before the Ehrenfest time. For larger times the evolution

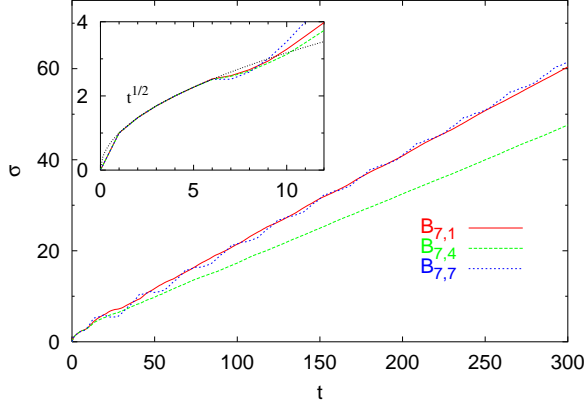


Figure 6: Standard deviation as a function of time for the environment of 7 qubits ($B_{7,n}$ with $n = 1, \dots, 7$) and $\eta = \kappa = 0.5$ in logarithmic scale. The particle was localized in position and the initial state of the environment is $|\phi_0\rangle = \frac{1}{\sqrt{2}}(|0\rangle + i|1\rangle)$ for each qubit

is more complex. For the regular environment the growth is clearly linear signalling a transition from classical to quantum, as expected. The behavior for chaotic evolutions is harder to visualize. At first glance the behavior of the SD seems to be linear with time. However, there is a clear separation between the slope of the line which is attained for the regular case and for the chaotic one being substantially smaller for the latter. Moreover we observe that by enlarging the dimensionality of the environment the slope of the SD for the chaotic environment decreases (while it remains constant for the regular case). The behavior of the slope (the time derivative of the SD) is displayed in Figure 7. The conclusion is that for large chaotic environments the time derivative of the variance tends to very small values as D increases. Therefore, the growth of the variance will be slower than linear, which is a manifestation of their larger efficiency as compared with regular ones.

The behavior of the variance for the regular map can be understood by generalizing some of the results obtained in [17] to include arbitrary Floquet angles in the Fourier transform. Then, one can show that the long time behavior of the variance is (for $|0\rangle$ position as initial state with $\eta = \kappa = 0$)

$$\sigma^2(t) = \frac{3 - 2\sqrt{2} + 1/N}{4\sqrt{2}} t^2 + O(t) + (\text{oscillatory terms}) \quad (14)$$

where N is the number of coins. One can show that changing Floquet angles is equivalent to changing the initial coin state [28]. Using this we obtained results which show that for long times the time derivative of the variance approaches a constant value for large number of qubits.

C. Approach to classical phase space distributions.

Another interesting aspect of the quantum to classical transition is the study of the way in which quantum phase space quasi-distributions (like Wigner functions [25]) approach

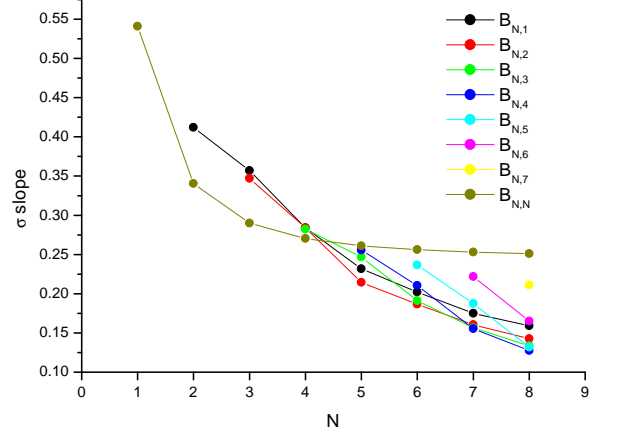


Figure 7: The time derivative of the standard deviation σ for long times as a function of the number of qubits in the environment. For regular dynamics the slope approaches a constant while for chaotic ones it decays. Thus, the position variance grows slower than linear for long periods of time, which is evidence in favor of the higher efficiency of chaotic environments.

their classical counterparts [26]. To study this we use the discrete version of the Wigner function [27]. For a system with an M -dimensional Hilbert space the discrete Wigner function can be defined in a phase space grid of $2M \times 2M$ points. Thus, the Wigner function is the expectation value of the so-called phase-space point operators which are defined as $A(q, p) = U^q R V^{-p} \exp(i\pi pq/M)$. Here U and V are the cyclic shift operator in position and momentum respectively ($U|n\rangle = |n+1\rangle$ and $V|k\rangle = |k+1\rangle$), and R is the reflection operator (which in the position basis acts as $R|n\rangle = |-n\rangle$). Phase-space operators are unitary, Hermitian and form a complete orthogonal basis of the space operators. As mentioned above, the Wigner function is defined as $W(q, p) = \text{Tr}[\rho A(q, p)]/M$. This function not only provides a complete description of the quantum state but also can be used to compute marginal probability distributions by adding its values along arbitrary phase space lines (see [27]). To study how fast the quantum state approaches a classical distribution we define a distance between two such distributions as $\delta_{1,2} \equiv \sum_{q,p} (W_1(q, p) - W_2(q, p))^2$. We analyze the distance between the Wigner function at any given instant and the classical distribution corresponding to the classical random walk. The behavior of this measure is displayed in Figure 8 for some representative members of the $B_{7,n}$ family. It can be seen that the regular map ($B_{7,7}$) significantly differs with respect to the chaotic maps. Again the most decoherence is attained by the chaotic environment. While interacting with the regular environment, the quantum state of the system loses track of the classical state after a short time. These results are in agreement with the ones obtained for the entropy and the position variance.

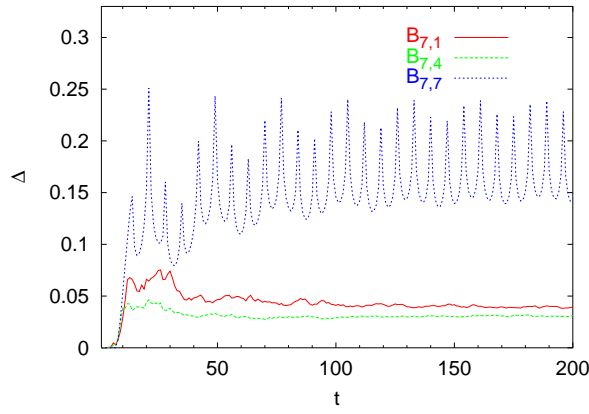


Figure 8: Evolution of phase-space distance (δ) for $B_{7,n}$ with $n = 1, \dots, 7$ and $\eta = \kappa = 0.5$. The particle was localized in position and the initial state of the environment is $\frac{1}{\sqrt{2}}(|0\rangle + i|1\rangle)$ for each qubit

IV. CONCLUSIONS

We studied a model where the decoherence induced on a system by its interaction with an environment can be analyzed both for an environment endowed with a regular or a chaotic evolution. As the Hilbert space of the environment has a finite dimension D , the system cannot display a truly dissipative behavior. In fact, after a finite time the environment ceases to be effective. For this reason, after this time quantum effects on the system can be recovered. Our results provide a strong evidence showing that a chaotic environment can be efficient over much longer timescales than regular ones. In fact, the time over which a chaotic environment is effective seems to scale as a power of the Hilbert space dimension D . On the other hand, a regular environment is effective only for a much shorter timescale, which is of the order of the Eherenfest time $\log(D)$. For such short timescales both environment are truly indistinguishable from each other.

-
- [1] see *Quantum theory and measurement*, edited by J.A. Wheeler and W.H. Zurek, Princeton Univ. Press (1983).
 - [2] for a review see J. P. Paz and W. H. Zurek, in "Coherent matter waves, Les Houches Session LXXII", edited by R Kaiser, C Westbrook and F David, EDP Sciences, Springer Verlag (Berlin) (2001) 533-614; W. Zurek, *Rev. Mod. Phys.* **75**, 715 (2003).
 - [3] A. Nielsen y I. Chuang, *Quantum Computation and Quantum Information*, Cambridge University Press (2000).
 - [4] R.P. Feynman and F.L. Vernon, *Ann. Phys.* **24**, 118 (1963).
 - [5] A.O. Caldeira and A.J. Leggett, *Physica* **121A**, 587-616 (1983); *Phys. Rev. A* **31**, 1059 (1985).
 - [6] B.L. Hu, J.P. Paz and Y. Zhang, *Phys. Rev. D* **45**, 2843 (1992).
 - [7] J.R. Anglin, J.P. Paz and W.H. Zurek, *Phys. Rev. A* **53**, 4041 (1997).
 - [8] N.V. Prokof'ev and P.C.M. Stamp, *Rep. Prog. Phys.* **63**, 669 (2000).
 - [9] V.V. Dobrovitsky and H.A. De Raedt, *Phys. Rev. E* **67** 056702 (2003).
 - [10] F. Cucchietti, J.P. Paz and W.H. Zurek, *Decoherence from a spin environment*, e-print quant-ph/0508xxx.
 - [11] R. Blume-Kohout and W.H. Zurek, *Phys. Rev. A* **68**, 032104 (2003).
 - [12] D. Cohen and T. Kottos, *Phys. Rev. E* **69**, 55201 (2004).
 - [13] J. Kempe, *Contemporary Physics* **44**, 307-327 (2003), e-print quant-ph/0303081.
 - [14] T.A. Brun, H.A. Carteret and A. Ambainis, *Phys. Rev. A* **67**, 032304 (2003).
 - [15] C.C. López and J.P. Paz, *Phys. Rev. A* **68**, 052305 (2003).
 - [16] R. Shack and M.C. Caves, *Applicable Algebra in Engineering, Communication and Computing*, 10, 305 (2000).
 - [17] T.A. Brun, H.A. Carteret and A. Ambainis, *Phys. Rev. A* **67**, 052317 (2003).
 - [18] N.L. Balazs and A. Voros, *Ann. Phys.* **190** (1989) 1.
 - [19] M. Saraceno, *Ann. Phys.*, **199** (1990) 37.
 - [20] D.K. Wójcik and J.R. Dorfman, *Physica D*, **187**, 223-243 (2004).
 - [21] A.J. Scott y M.C. Caves, *J. Phys. A* **36** 9553 (2003), quant-ph/0305046 (2003).
 - [22] L. Ermann and M. Saraceno in preparation.
 - [23] "*Quantum theory concepts and methods*", A. Peres, Kluwer Univ. Press (1994); see Chapter 12.
 - [24] H. Pastawski, G. Usaj, and P. Levstein, *Chem. Phys. Lett.* **261** 329 (1996); R. Jalabert and H. Pastawski, *Phys. Rev. Lett.* (2001); F. Cucchietti, D. Dalvit, J.P. Paz and W.H. Zurek, *Phys. Rev. Lett.* **91** 210403 (2003).
 - [25] M. Scully, M. Hillery and E. Wigner, *Phys. Rep.* **106**, 121 (1984).
 - [26] J.P. Paz, S. Habib and W.H. Zurek, *Phys. Rev. D* **47**, 488 (1993).
 - [27] C. Miquel, J.P. Paz, M. Saraceno, *Phys. Rev. A* **65**, 062309 (2002).
 - [28] E. Bach, S. Coppersmith, M.P. Goldschen, R. Joynt, J. Watrous (2002) e-print quant-ph/0207008.